Reduced first-order density matrices and "exchange-only" correlation factors for some closed-shell atomic systems

Shridhar R. Gadre and Sudhir A. Kulkarni
Department of Chemistry, University of Poona, Pune-411007, Maharashtra, India

Rajeev K. Pathak
Department of Physics and Department of Chemistry, University of Poona, Pune-411007, Maharashtra, India
(Received 6 December 1988)

Systematic investigations on the structure of the reduced, first-order atomic density matrices and the "exchange-only" correlation factors within the frameworks of the Hartree-Fock theory, local-density approximation, and nonlocal-density approximation (NLDA) are carried out. The contours of suitably averaged density matrices and correlation factors for some closed-shell atomic systems are plotted and compared, clarifying some of their significant general features. Exchange energies within the NLDA scheme for these systems have also been computed.

I. INTRODUCTION

An atomic, molecular, or solid-state N-electron bound system with Coulombic interactions is described by the Hamiltonian

$$\hat{H}=\hat{T}+\hat{U}+\hat{V}_{\text{ext}} \tag{1}$$

with the kinetic energy operator $T=-\frac{1}{2}\sum_i \nabla_i^2$, the electron-electron repulsion $U=\sum_{i<j=1}^{N} 1/r_{ij}$, and the external binding local potential $\hat{V}_{\text{ext}}=\sum_i v_{\text{ext}}(\mathbf{r}_i)$. [Hartree atomic units, i.e., $\hbar=m_e=|e|=1$ (numerically), are used throughout.]

For such a system, with spin-free interactions, the ground-state physical properties can be derived with the knowledge, at most, of the diagonal part of the second-order spinless density matrix, $\Gamma^{(2)}(\mathbf{r}_1,\mathbf{r}_2|\mathbf{r}_1,\mathbf{r}_2)$. In general,[1] the pth order spinless density matrix is defined by

$$\Gamma^{(p)}(\mathbf{r}_1,\mathbf{r}_2,\ldots,\mathbf{r}_p|\mathbf{r}'_1,\mathbf{r}'_2,\ldots,\mathbf{r}'_p)=\binom{N}{p}\sum_{\sigma_1,\sigma_2,\ldots,\sigma_N}\cdots\sum_{\sigma'_1,\sigma'_2,\ldots,\sigma'_p}\int\Psi^*(\mathbf{x}_1,\mathbf{x}_2,\ldots,\mathbf{x}_p,\mathbf{x}_{p+1},\ldots,\mathbf{x}_N)\times\Psi(\mathbf{x}'_1,\mathbf{x}'_2,\ldots,\mathbf{x}'_p,\mathbf{x}_{p+1},\ldots,\mathbf{x}_N)\times d\mathbf{r}_{p+1}\cdots d\mathbf{r}_N\ , \tag{2}$$

where $\mathbf{x}$ is the space-spin index: $\mathbf{x}\equiv(\mathbf{r},\sigma)$. Within the Hartree-Fock (HF) theory for closed-shell systems, $\Gamma^{(2)}(\mathbf{r}_1,\mathbf{r}_2|\mathbf{r}_1,\mathbf{r}_2)$ can be exactly decomposed as[2]

$$2\Gamma^{(2)}_{\text{HF}}(\mathbf{r}_1,\mathbf{r}_2|\mathbf{r}_1,\mathbf{r}_2)=\rho_{\text{HF}}(\mathbf{r}_1)\rho_{\text{HF}}(\mathbf{r}_2)-\Gamma^{(1)}_{\text{HF}}(\mathbf{r}_1|\mathbf{r}_2)\Gamma^{(1)}_{\text{HF}}(\mathbf{r}_2|\mathbf{r}_1)/2\ , \tag{3}$$

with the closed-shell HF first-order density matrix $\Gamma^{(1)}_{\text{HF}}$ given by

$$\Gamma^{(1)}_{\text{HF}}(\mathbf{r}_1|\mathbf{r}_2)=2\sum_i u_i^*(\mathbf{r}_1)u_i(\mathbf{r}_2)\ . \tag{4}$$

Here, the u_i's denote the canonical HF orbitals. The one-electron density $\rho(\mathbf{r})$ is given by $\rho(\mathbf{r})=\Gamma^{(1)}(\mathbf{r}|\mathbf{r})$, in general. Thus, within the realm of HF, for closed-shell systems, the status of fundamentality is endowed to $\Gamma^{(1)}_{\text{HF}}(\mathbf{r}|\mathbf{r}')$, through which all ground-state physical properties may be extracted. The Hartree-Fock theory takes into account the "exchange-only" correlations among electrons with parallel spin orientations, from which the "exchange-only" correlation factor $C^{\text{HF}}_{\text{exch}}(\mathbf{r}_1,\mathbf{r}_2)$ emerges[2]

$$2\Gamma^{(2)}_{\text{HF}}(\mathbf{r}_1,\mathbf{r}_2|\mathbf{r}_1,\mathbf{r}_2)=\rho_{\text{HF}}(\mathbf{r}_1)\rho_{\text{HF}}(\mathbf{r}_2)[1+C^{\text{HF}}_{\text{exch}}(\mathbf{r}_1,\mathbf{r}_2)]\ . \tag{5}$$

Thus, from Eqs. (3)–(5),

$$C^{\text{HF}}_{\text{exch}}(\mathbf{r}_1,\mathbf{r}_2)=-|\Gamma^{(1)}_{\text{HF}}(\mathbf{r}_1|\mathbf{r}_2)|^2/[2\rho_{\text{HF}}(\mathbf{r}_1)\rho_{\text{HF}}(\mathbf{r}_2)]\ . \tag{5'}$$

The Hartree-Fock exchange energy is then given by

$$E^{\text{HF}}_{\text{exch}}=\tfrac{1}{2}\int\rho_{\text{HF}}(\mathbf{r}_1)Q_{\text{exch}}(\mathbf{r}_1,\mathbf{r}_2)|\mathbf{r}_1-\mathbf{r}_2|^{-1}d\mathbf{r}_1 d\mathbf{r}_2\ ,$$

where

$$Q_{\text{exch}}=\rho_{\text{HF}}(\mathbf{r}_2)C^{\text{HF}}_{\text{exch}}(\mathbf{r}_1,\mathbf{r}_2)$$

is the "exchange hole."

The HF "exchange-only" correlation factor $C_{\rm exch}$ must satisfy the following properties ($C^{\rm HF}_{\rm exch} \equiv C_{\rm exch}$):

$$\lim_{|\mathbf{r}_1-\mathbf{r}_2|\to\infty} C_{\rm exch}(\mathbf{r}_1,\mathbf{r}_2)=0 \ , \tag{6a}$$

$$\lim_{\mathbf{r}_1\to\mathbf{r}_2} C_{\rm exch}(\mathbf{r}_1,\mathbf{r}_2)=-\tfrac{1}{2} \ , \tag{6b}$$

$$\int C_{\rm exch}(\mathbf{r}_1,\mathbf{r}_2)\rho_{\rm HF}(\mathbf{r}_2)d\mathbf{r}_2=\int Q_{\rm exch}(\mathbf{r}_1,\mathbf{r}_2)d\mathbf{r}_2 = -1, \quad \text{for all } \mathbf{r}_1 \tag{6c}$$

and

$$\lim_{\rho\to\rho_0=\text{const}} C_{\rm exch}(\mathbf{r}_1,\mathbf{r}_2)=C^{H}_{\rm exch}(\mathbf{r}_1,\mathbf{r}_2) \ , \tag{6d}$$

where $C^{H}_{\rm exch}(\mathbf{r}_1,\mathbf{r}_2)$ represents the exchange-only-correlation factor for a homogeneous electron gas of density ρ_0. The exact form of $C^{H}_{\rm exch}(\mathbf{r}_1,\mathbf{r}_2)$ is known:[3,4]

$$C^{H}_{\rm exch}(\mathbf{r}_1,\mathbf{r}_2)=-\tfrac{9}{2}[j_1(y_0)/y_0]^2 \tag{7}$$

with $y_0=k_F^{(0)}|\mathbf{r}_1-\mathbf{r}_2|$, $k_F^{(0)}=(3\pi^2\rho_0)^{1/3}$, and j_1, the first-order spherical Bessel function:

$$j_1(y)=[\sin(y)-y\cos(y)]/y^2 \ .$$

A popular approximation, namely, the local-density approximation[3] (LDA) consists of using the form (7) even when the density $\rho(\mathbf{r})$ is inhomogeneous. This is achieved by the replacement $k_F^{(0)}\to k_F(\mathbf{r})$, $\rho_0\to\rho(\mathbf{r})$. Such a simplification leads to a reasonable estimate of the exchange energy[3,4]

$$E_{\rm exch}\simeq -\tfrac{3}{4}(3/\pi)^{1/3}\int \rho^{4/3}(\mathbf{r})d\mathbf{r} \ . \tag{8}$$

However, such an average description violates[2] the "Fermi (or, exchange) hole condition" (6c); also, the Hermiticity of the correlation factor is lost.

In order to better simulate the realistic systems, Slater[4] introduced a multiplicative parameter α in the approximation (8). The values of α were chosen to be atom (or molecule) dependent. Gopinathan *et al.*[5] devised a scheme to compute the spin-dependent α values $(\alpha_\uparrow,\alpha_\downarrow)$ for atomic systems, employing a linear approximation to the spherically symmetric Fermi hole.[5] Within the density functional[6–8] framework, Perdew and Zunger[9] introduced a "self-interaction correction" (SIC) to the local-spin-density[9] (LSD) approximation (within the Kohn-Sham[7] regime) so that for the same orbital with a given spin, the classical Coulomb and exchange-energy contributions were made to exactly cancel each other, which, of course, happens naturally within the HF theory. Perdew and Zunger[9] also plotted the exchange hole $Q_{\rm exch}(\mathbf{r}_1,\mathbf{r}_2)$ for some chosen values of $\mathbf{r}_1$ for the case of neon with $\mathbf{r}_2$ orientations parallel to $\mathbf{r}_1$. They demonstrated that the shape of the exchange hole for the LSD-SIC case mimics the corresponding HF one very well, whereas the "LSD-only" hole very poorly represents it. A study on the shapes of HF Coulomb[10] and exchange[9,11] holes was carried out by several workers.

In their alternative approach to correct for the LSD approximation, Alonso and Girifalco[2] introduced a nonlocal-density approximation (NLDA) through which the condition (6c) was restored through the prescription

$$C^{\rm NLDA}_{\rm exch}[\tilde\rho(\mathbf{r}_1),|\mathbf{r}_1-\mathbf{r}_2|]=-\tfrac{9}{2}[j_1(\tilde y)/\tilde y]^2 \tag{9}$$

with $\tilde y=\tilde k_F(\mathbf{r}_1)|\mathbf{r}_1-\mathbf{r}_2|$,

$$\tilde k_F(\mathbf{r}_1)=[3\pi^2\tilde\rho(\mathbf{r}_1)]^{1/3} \ .$$

In Eq. (9), $\tilde\rho$ is determined at all points $\mathbf{r}_1$ via

$$\int C^{\rm NLDA}_{\rm exch}[\tilde\rho(\mathbf{r}_1),|\mathbf{r}_1-\mathbf{r}_2|]\rho(\mathbf{r}_2)d\mathbf{r}_2=-1 \ .$$

The density matrix within the LDA regime thus turns out to be

$$\Gamma^{(1)}_{\rm LDA}(\mathbf{r}_1|\mathbf{r}_2)=\rho^{1/2}(\mathbf{r}_1)\rho^{1/2}(\mathbf{r}_2)[3j_1(y)/y] \tag{10}$$

and analogously,

$$\Gamma^{(1)}_{\rm NLDA}(\mathbf{r}_1|\mathbf{r}_2)=\rho^{1/2}(\mathbf{r}_1)\rho^{1/2}(\mathbf{r}_2)[3j_1(\tilde y)/\tilde y] \ . \tag{11}$$

One of the attractive features brought about by NLDA is the following: Starting exclusively from a given density distribution $\rho(\mathbf{r})=\Gamma^{(1)}(\mathbf{r}|\mathbf{r})$, NLDA enables one to obtain satisfactory approximations[12,13] to the *full* first-order density matrix $\Gamma^{(1)}(\mathbf{r}|\mathbf{r}')$. Upon Fourier transformation of this $\Gamma^{(1)}(\mathbf{r}|\mathbf{r}')$ one is able to obtain reasonable (as compared to the HF quantities) estimates of the first-order density matrix in momentum space[12] viz., $\Gamma^{(1)}_{\rm mom}(\mathbf{p}|\mathbf{p}')$, and consequently the atomic or molecular momentum density $\gamma(\mathbf{p})=\Gamma^{(1)}_{\rm mom}(\mathbf{p}|\mathbf{p})$, as well as the Compton profile.[13] Gadre *et al.*[12,13] further harnessed the nonlocal-density approximation to extract estimates of kinetic-energy anisotropies[13] and the directional Compton profiles[12] employing the molecular $\rho(\mathbf{r})$ as a starting point.

The success of the nonlocal-density approximation prompts one to compare the density matrices and correlation factors within LDA and NLDA with their HF counterparts. All the earlier studies carried out[11] for the portrayal of $\Gamma^{(1)}$ and $C_{\rm exch}$ employed the following strategy: Take a fixed point $\mathbf{r}_1$ and move $\mathbf{r}_2$ parallel to $\mathbf{r}_1$ and obtain the curves for $\Gamma^{(1)}(r_1|r_2)$ or $C_{\rm exch}(r_1,r_2)$ where r_1 and r_2 denote $|\mathbf{r}_1|$ and $|\mathbf{r}_2|$, respectively. Incidentally, Weyrich[14] has recently presented contours of $\Gamma^{(1)}(\mathbf{r}|\mathbf{r}')$ using HF quality wave functions for small organic molecules.

In this article, a different and more general approach is adopted. Different *contours* of spherically averaged $\Gamma^{(1)}(\mathbf{r}_1|\mathbf{r}_2)|$ as well as those of $C_{\rm exch}(\mathbf{r}_1,\mathbf{r}_2)$ are drawn and compared, on the same footing, with those within the LDA, NLDA, and HF domains. For such a study, selected close-shell atomic systems, viz., Be, Ne, Mg, Ar, Ca, and Kr are considered. Further, the exchange energies for these species within NLDA are computed and compared with the LDA and HF exchange energies.

II. DENSITY MATRICES

For notational convenience $\Gamma^{(1)}(\mathbf{r}|\mathbf{r}')$ will be written as $\Gamma(\mathbf{r}|\mathbf{r}')$. For the closed-shell atoms mentioned earlier, the

density matrix $\Gamma(\mathbf{r}|\mathbf{r}')$ and the "exchange-only" correlation factor $C_{\text{exch}}(\mathbf{r},\mathbf{r}')$ computed within the three regimes, viz., HF, LDA, and NLDA, are displayed. For the HF part, the near Hartree-Fock (NHF) quality wave functions with Slater-type-orbital (STO) bases tabulated by Clementi and Roetti[15] were chosen. For the purpose of portrayal of Γ_{HF} and $C_{\text{exch}}^{\text{HF}}$, we take only the normalized radial part of the HF orbitals. This is equivalent to the prescription

$$\Gamma_{\text{HF}}(r|r') \equiv \int [\Gamma_{\text{HF}}(\mathbf{r}|\mathbf{r}')]_{\theta'=\theta,\phi'=\phi}(4\pi)^{-1}d\Omega \ , \tag{12}$$

for spherically symmetrizing the density matrix, whence the HF exchange-only-correlation factor becomes

$$C_{\text{exch}}^{\text{HF}}(r,r') = -[\Gamma_{\text{HF}}(r|r')]^2/[2\rho_{\text{HF}}(r)\rho_{\text{HF}}(r')] \ . \tag{13}$$

Note that the quantities on the left-hand sides of Eqs. (12) and (13) are spherically symmetric in the primed and unprimed variables. The figures depict the contours of $\Gamma(\mathbf{r}|\mathbf{r}')$ and $C_{\text{exch}}(\mathbf{r},\mathbf{r}')$, i.e., loci of $\Gamma(\mathbf{r}|\mathbf{r}')=$const and $C_{\text{exch}}(\mathbf{r},\mathbf{r}')=$const with the HF description as a standard. As to the contours of Γ within the LDA and NLDA theories, note that the dependences are on $|\mathbf{r}|$ and $|\mathbf{r}-\mathbf{r}'|$, hence, for plotting, we choose $\mathbf{r}$ parallel to $\mathbf{r}'$. For the contours of $\Gamma_{\text{HF}}(r|r')$ given in Figs. 1–4, the following general salient features are noteworthy.

(1) The contours of $\Gamma_{\text{HF}}(r|r')$ are symmetric around $r=r'$, as they should be, since, in general, $\Gamma(\mathbf{r}|\mathbf{r}')=\Gamma^*(\mathbf{r}'|\mathbf{r})$ by Hermiticity in conjunction with the reality of the NHF orbitals, by construction.

(2) The negative-valued contours of Γ_{HF} ought to be multiply connected, as they can *never* cross the line $r=r'$ because $\Gamma(\mathbf{r}|\mathbf{r})=\rho(\mathbf{r})\geq 0$.

(3) For small values of both r and r', one expects a linear behavior. This follows from the fact that only s-type STO's contribute significantly to Γ for small values of r and r', whence

$$\Gamma_{\text{HF}}(r|r') \sim e^{-\alpha r}e^{-\beta r'} = 1-\alpha r-\beta r'+O(r^2)+O(r'^2) \ .$$

(Here α,β denote the typical exponents for s-type STO's.) The symmetry of $\Gamma(\mathbf{r}|\mathbf{r}')$ demands that such contours will be almost linear, *making equal intercepts* on the axes.

(4) For increasing values of r and r' the contours become curved in general. Further, if a tangent to the con-

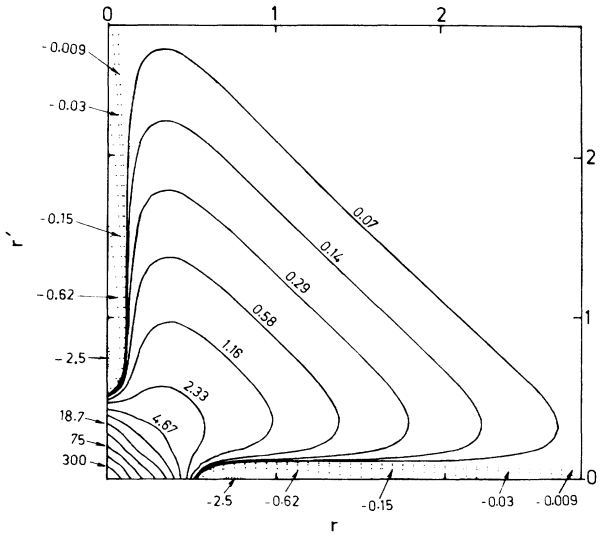

FIG. 2. Contours of the spherically averaged Hartree-Fock density matrix for neon. The successive contour values differ by a factor of 2 for the positive-valued contours and by a factor of 4 for the negative-valued ones.

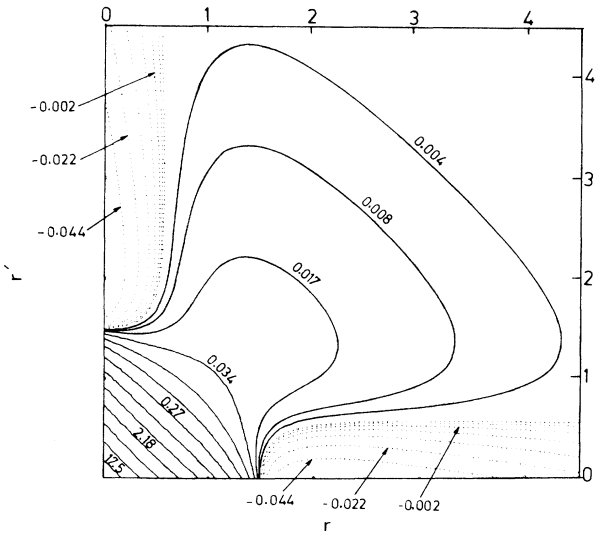

FIG. 1. Contours of the spherically averaged density matrix for beryllium within the Hartree-Fock theory. The successive contour values differ by a factor of 2 both for positive- as well as negative-values contours.

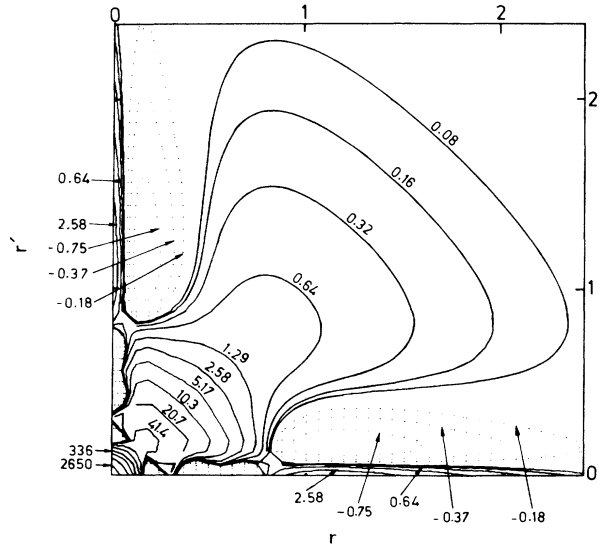

FIG. 3. Contours of the spherically averaged Hartree-Fock density matrix for calcium. The neighboring contour values differ by a factor of 2 both for positive- and negative-valued contours.

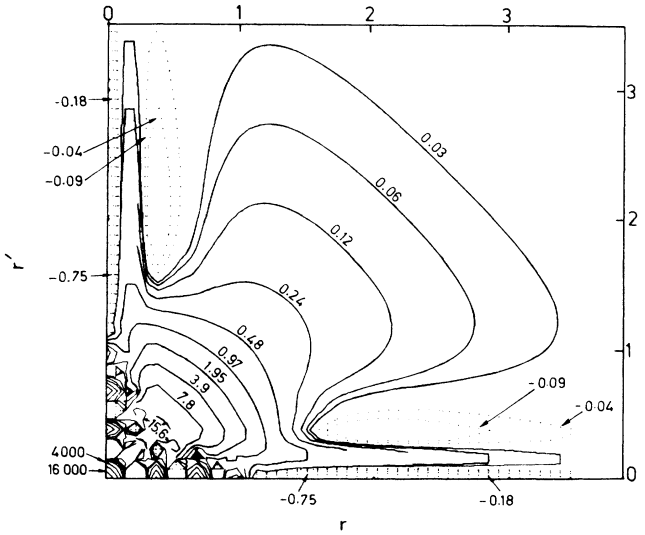

FIG. 4. Contours of the spherically averaged Hartree-Fock density matrix for krypton. The successive contour values differ by a factor of 2. Note the rich, complex structure of the density matrix (see text for further details).

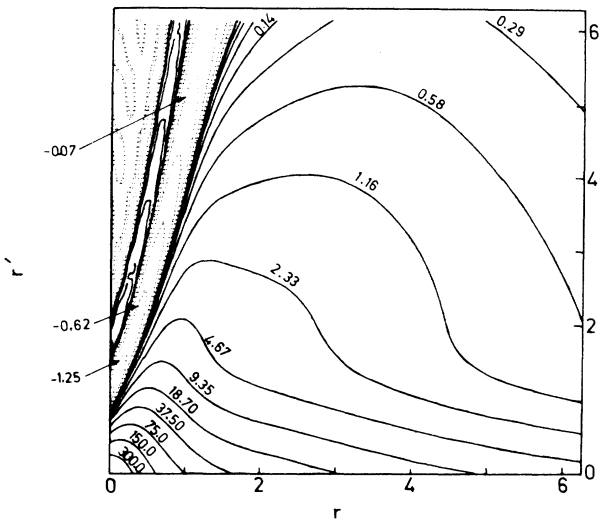

FIG. 5. Contours of the density matrix within the local-density approximation for neon. The neighboring contour values differ by a factor of 2. The directions of **r** and **r'** are parallel.

tour is drawn at $r=r'$, it is observed that the contour (that has to be positive valued) entirely lies in the region bounded by the tangent and the r and r' axes. Thus, around $r=r'$, the contours are convex as seen from the increasing $r(=r')$ side.

(5) For large values of both r and r' (in principle, when both r and $r'\to\infty$), $\Gamma(r|r')$ is represented as[16]

$$\Gamma(r|r')=[\rho(r)\rho(r')]^{1/2}$$

(for a positive-valued Γ). Thus, for extremely large r and r' values, $\rho(r)\sim r^{l}e^{-\alpha r}$. Also $\Gamma\geq 0$ for $r=r'$. Hence,

$$\ln\Gamma(r|r')\sim l[\ln(r)+\ln(r')]-\alpha(r+r') .$$

Also, for very large r values, $r\gg\ln(r)$, hence, for a contour of Γ, $\alpha(r+r')\sim$const leading to a linear behavior, a feature clearly discernible in the plots of $\Gamma(r|r')$ for asymptotic values of r and r'.

Among the studies carried out, beryllium ($N=Z=4$) exhibits the simplest $\Gamma(r|r')$ plot. Note that, for Be, only the ψ_{2s}^{HF} is seen to possess a prominent $2s$-orbital node,[17] which occurs around $r=0.75$. Thus, in the region $r>0.75$, $r'>0.75$ one never encounters negative-valued contours as is borne out by Fig. 1. In general, the occurrence of the negative-valued contours is a cumulative effect of the nodal structure which arises out of the orthogonality of the radial wave functions. Thus, for Ne (where $2s$ is the only orbital that has a prominent node), the negative region appreciably shrinks towards the r and r' axes (see Fig. 2). It also turns out that in all the Γ plots, the negative-valued contours occupy a very small fraction of the total diagram.

For both Ne and Ar, the positive contours are seen to flatten around $r=r'$ for large enough r and r' in accordance with (5) above. However, for Ar, the negative region becomes significant, owing to the inclusion of $3s$ and $3p$ orbitals that give rise to the nodes. Petal-like structures representing closed contours for the negative part for Ar, Ca, as well as Kr, are conspicuous; only the last two among these are displayed in Figs. 3 and 4, respectively.

For Mg and Ca, positive contours show an appreciable curvature as compared to their counterparts for Ne and Ar, respectively. For Mg, the negative part is almost

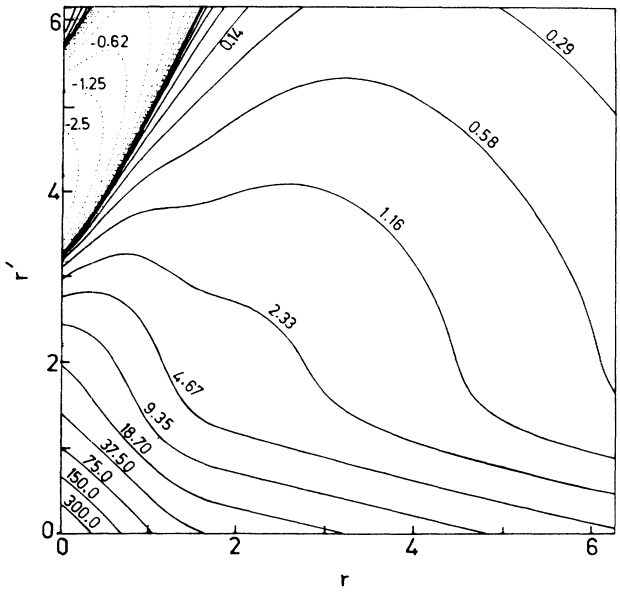

FIG. 6. Contours of the density matrix for neon within the nonlocal-density approximation. The successive contour values differ by a factor of 2. The directions of **r** and **r'** are parallel.

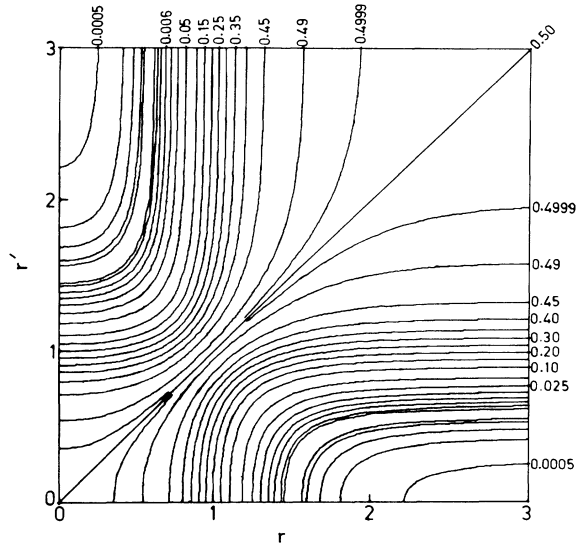

FIG. 7. Contours of the negative of the Hartree-Fock "exchange-only" correlation factor, i.e., $-C^{\mathrm{HF}}_{\mathrm{exch}}(r,r')$, for beryllium.

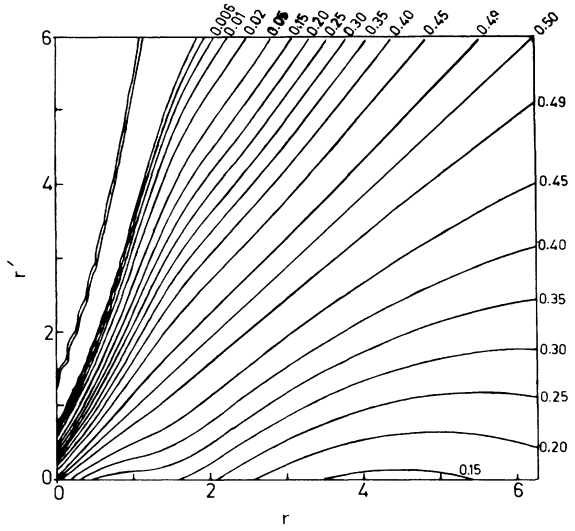

FIG. 9. Contours of $-C^{\mathrm{LDA}}_{\mathrm{exch}}(\mathbf{r},\mathbf{r}')$, the negative of the "exchange-only" correlation factor, for neon within the local-density approximation. The directions of $\mathbf{r}$ and $\mathbf{r}'$ are parallel.

insignificant which is attributed to a sizable positive contribution from the nodeless $2p$ orbital augmented by the $3s$ positive contribution which is overwhelmingly larger than its negative one. The above features are noticeable from the contour plot for Mg, which cannot be presented here due to paucity of space.

The contours for Kr exhibit a complicated structure, with an alternative interlacing of the positive- and negative-valued contours, around $r \approx r' \approx 0$ (cf. Fig. 4).

The contours of $\Gamma_{\mathrm{LDA}}(\mathbf{r}|\mathbf{r}')$, as well as $\Gamma_{\mathrm{NLDA}}(\mathbf{r}|\mathbf{r}')$, do not exhibit the symmetry and the rich structure as in the case of $\Gamma_{\mathrm{HF}}(r|r')$. For the respective r and r' ranges chosen, the negative region is lopsided both within LDA and NLDA. Contours of Γ_{LDA} and Γ_{NLDA} for Ne as a representative case are drawn in Figs. 5 and 6, respectively. The Γ_{NLDA} contours mimic their HF counterparts for $r \approx r' \approx 0$ (linear behavior), a feature absent for the LDA case. Also, the Γ_{LDA} contours, in general, exhibit a greater curvature than those within NLDA. Owing to their very complicated implicit dependence on the density, the LDA and NLDA curves elude any systematic *general* investigation.

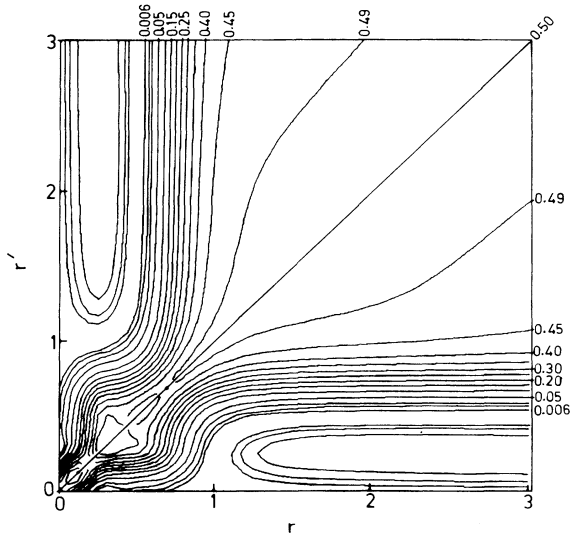

FIG. 8. Contours of the negative of the Hartree-Fock "exchange-only" correlation factor, i.e., $-C^{\mathrm{HF}}_{\mathrm{exch}}(r,r')$, for argon.

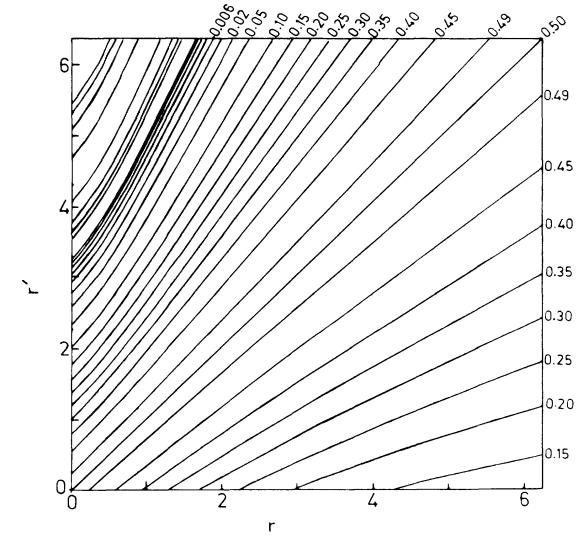

FIG. 10. Contours of $-C^{\mathrm{NLDA}}_{\mathrm{exch}}(\mathbf{r},\mathbf{r}')$, the negative of the "exchange-only" correlation factor, for neon within the nonlocal-density approximation. The directions of $\mathbf{r}$ and $\mathbf{r}'$ are parallel.

III. EXCHANGE-CORRELATION FACTORS AND EXCHANGE ENERGIES

A discussion of contours of $\Gamma(\mathbf{r}|\mathbf{r}')$ has been presented in the previous section. It is also instructive to examine the contours of $C^{\rm HF}_{\rm exch}(r,r')$. As to the contours of the (exchange-only) correlation factor $C^{\rm HF}_{\rm exch}(r,r')$, observe that there is a good deal of detail and symmetry within the realm of HF (see Figs. 7 and 8 for Be and Ar, respectively), which is lost in the LDA and NLDA descriptions (cf. Figs. 9 and 10 for the case of Ne). As the $C_{\rm exch}$ factors within the LDA and NLDA regimes depend on $|\mathbf{r}|$ and $|\mathbf{r}-\mathbf{r}'|$, Figs. 9 and 10 are drawn with specific directions of $\mathbf{r}$ and $\mathbf{r}'$, viz., $\mathbf{r}$ being parallel to $\mathbf{r}'$. In fact, the curvature evinced by the $C^{\rm NLDA}_{\rm exch}$ contours is very small in comparison with the LDA ones as displayed in Figs. 9 and 10. Also, it is evident that LDA and NLDA theories do not adequately represent the HF exchange hole locally, even though gross quantities such as the exchange-energy estimates, as compared to the HF values, are approximated rather well.[3,4] The reason for the loss of detail in the NLDA case is attributed to absence of the orbitals and $\tilde{\rho}^{1/3}(r)$ being a nodeless, as well as a rather slowly varying, quantity [cf. Eq. (9)]. It is also noted that $C^{\rm NLDA}_{\rm exch}(\mathbf{r},\mathbf{r}')$ mimics its HF counterpart well for both small r and r' values. The overall similarity between contours for LDA and NLDA for a given species is remarkable as can be inferred from Figs. 9 and 10. Unlike the factor $C^{\rm HF}_{\rm exch}$, the correlation factors $C^{\rm LDA}_{\rm exch}$ and $C^{\rm NLDA}_{\rm exch}$ are inherently asymmetric; however, an attempt to force the symmetrization in to $C^{\rm LDA}_{\rm exch}$ in an *ad hoc* manner only worsens the exchange-energy[18] estimates. That the NLDA is an improvement over LDA follows from the $E^{\rm NLDA}_{\rm exch}$ values lying closer to $E^{\rm HF}_{\rm exch}$ than do the $E^{\rm LDA}_{\rm exch}$ values for prechosen[15] NHF electron densities.

The exchange energies within NLDA can be obtained setting

$$C^{\rm NLDA}_{\rm exch}(\mathbf{r}_1,\mathbf{r}_2)\equiv C_{\rm exch}(r_1,r_{12})$$
$$=-\tfrac{9}{2}j_1^2\{[3\pi^2\tilde{\rho}(r_1)]^{1/3}r_{12}\}/\{[3\pi^2\tilde{\rho}(r_1)]^{1/3}r_{12}\}^2$$

and performing the integration after Eq. (5)

$$E^{\rm NLDA}_{\rm exch}=\int\rho(r_1)\rho(r_2)C_{\rm exch}(r_1,r_{12})(2r_{12})^{-1}d\mathbf{r}_1d\mathbf{r}_2\ .$$

Transforming the six-dimensional volume element $d\mathbf{r}_1d\mathbf{r}_2$ to the metric coordinate system on the lines of Coulson and Nielson:[19]

$$d\mathbf{r}_1d\mathbf{r}_2=r_1r_2r_{12}\sin\theta_1d\theta_1dr_1dr_2d\phi_1d\chi \tag{14}$$

and integrating over the angles θ_1 (in the interval $[0,\pi]$) and ϕ,χ (in the interval $[0,2\pi]$) one arrives at

$$E^{\rm NLDA}_{\rm exch}=4\pi^2\int_{\Delta(r_1,r_2,r_{12})}\rho(r_1)\rho(r_2)C_{\rm exch}(r_1,r_{12})r_1r_2dr_1dr_2\ , \tag{15}$$

where the condition $\Delta(r_1,r_2,r_{12})$ indicates that r_1, r_2, and r_{12} form a triangle, thus $|r_1-r_2|\le r_{12}\le r_1+r_2$. Hence

$$E^{\rm NLDA}_{\rm exch}=4\pi^2\int_{r_1=0}^{r_1=\infty}r_1\rho(r_1)dr_1\int_{r_2=r_1}^{r_2=\infty}r_2\rho(r_2)dr_2\left[\int_{r_{12}=r_2-r_1}^{r_{12}=r_2+r_1}C_{\rm exch}(r_1,r_{12})dr_{12}\right]$$
$$+4\pi^2\int_{r_1=0}^{r_1=\infty}r_1\rho(r_1)dr_1\int_{r_2=0}^{r_2=r_1}r_2\rho(r_2)dr_2\left[\int_{r_{12}=r_1-r_2}^{r_{12}=r_1+r_2}C_{\rm exch}(r_1,r_{12})dr_{12}\right]\ . \tag{16}$$

TABLE I. Exchange energies $E_{\rm exch}$ for some selected closed-shell atoms within the LDA, NLDA, and HF theories[a] (values in Hartree a.u.).

Atom	$-E^{\rm LDA}_{\rm exch}$	$-E^{\rm NLDA}_{\rm exch}$	$-E^{\rm HF}_{\rm exch}$	LDA error[b] (%)	NLDA error[b] (%)
Be	2.313	2.561	2.670	13.5	4.1
Ne	11.03	12.09	12.13	9.1	0.3
Mg	14.61	15.25	16.02	8.8	4.8
Ar	27.87	28.65	30.30	8.0	5.4
Ca	32.59	33.58	35.35	7.9	5.1
Kr	88.63	91.05	94.63	6.3	3.8

[a]See text for further details.

[b]Percent errors defined with respect to the corresponding HF values obtained from the NHF wave functions of Ref. 15.

The exchange energies for closed-shell atoms within NLDA along with corresponding HF and LDA values are displayed in Table I. From this table, one notices a numerical ordering: $E_{\text{exch}}^{\text{HF}} < E_{\text{exch}}^{\text{NLDA}} < E_{\text{exch}}^{\text{LDA}}$, which evidently means that the NLDA exchange energies fall closer to the HF ones than do the corresponding LDA values. The fair agreement between LDA and NLDA exchange energies with the HF values is thus on a gross scale, where the subtleties in the details of local structure of the exchange hole are obliterated.

IV. CONCLUDING REMARKS

In this paper, an attempt has been made to investigate the details of the atomic density matrices and the "exchange-only" correlation factors within the frameworks of Hartree-Fock, local-density approximation, and the nonlocal-density approximation. A clear connection with the earlier works of Boyd *et al.* and others[10,11] can be established as follows: In the plot for $C_{\text{exch}}^{\text{HF}}(r,r')$ contours, draw a line parallel to the r axis through a prechosen value of r'. The points of intersection, weighted by the density $\rho(r)$, would lead to the shapes of the exchange holes for a fixed electron coordinate as plotted in the studies cited above.

Further, it may be pointed out that the present analysis employs exclusively the STO basis sets tabulated by Clementi and Roetti.[15] Using other basis sets such as the popular Gaussian-type-orbital (GTO) basis, one would expect similar general features at a gross level. However, the STO's inherently possess two desirable characteristics rigorously satisfied by the exact wave function and the exact electronic density, respectively, viz., the "cusp condition" and "an asymptotic exponential falloff." The GTO's, being deprived of these properties, would give rise to a qualitatively different behavior of the contours for Γ and C_{exch} especially for the limiting and asymptotic values of r and r'. Moreover, beyond the Hartree-Fock approximation, one may employ the natural spin orbitals (NSO's), thereby making tangible the exact density matrix and the *full exchange-correlation* factor.

Systematic investigations on the density matrices and correlation factors within momentum space hitherto remain to be carried out except for some studies on the "correlation coefficients"[20] in momentum space[20,21] analogous to those for the position space[22] already reported in the literature. The density matrices in the coordinate and momentum spaces are connected via a six-dimensional Fourier-Dirac transformation. Thus, one expects complementary features exhibited by Γ and Γ_{mom} as demonstrated by Coulson[23] for their respective diagonal parts. The generalization of the present study to molecular[14] as well as solid-state systems is also straightforward. All these studies are being carried out in this laboratory.

ACKNOWLEDGMENTS

The financial assistance from the Department of Science and Technology (Scheme No. SP/S1/J00/85) and the University Grants Commission (UGC) [Scheme No. F.12-43/86 (SR III)], New Delhi, India, is gratefully acknowledged. S.A.K. further thanks UGC for financial support.

[1]See, for example, P.-O. Löwdin, Phys. Rev. **97**, 1474 (1955); **97**, 1490 (1955); **97**, 1509 (1955); A. J. Coleman, Rev. Mod. Phys. **35**, 668 (1963); T. Ando, *ibid.* **35**, 690 (1963); D. W. Smith, in *Reduced Density Matrices with Applications to Physical and Chemical systems,* edited by A. J. Coleman and R. M. Erdahl (Queen's University, Kingston, Canada, 1968).

[2]J. A. Alonso and L. A. Girifalco, Solid State Commun. **24**, 135 (1977); Phys. Rev. B **17**, 3735 (1978); for earlier work on the Hartree-Fock density matrices see, R. McWeeny, Rev. Mod. Phys. **32**, 335 (1960); P.-O. Löwdin, Adv. Phys. **5**, 1 (1956); J. Appl. Phys. **33**, 251 (1962).

[3]J. C. Slater, Phys. Rev. **81**, 385 (1951).

[4]J. C. Slater, *The Calculation of Molecular Orbitals* (Wiley, New York, 1979).

[5]M. S. Gopinathan, M. A. Whitehead, and R. Bogdanovic, Phys. Rev. A **14**, 1 (1976).

[6]P. Hohenberg and W. Kohn, Phys. Rev. **136B**, 864 (1964).

[7]W. Kohn and L. J. Sham, Phys. Rev. **140A**, 1133 (1965).

[8]See, for a review, in *Density Functional Methods in Physics,* Vol. 123 of *NATO Advanced Study Institute, Series B: Physics* edited by R. M. Dreizler and J. da Providencia (Plenum, New York, 1985).

[9]J. P. Perdew and A. Zunger, Phys. Rev. B **23**, 5048 (1981).

[10]R. J. Boyd, Can. J. Phys. **53**, 592 (1975); R. J. Boyd and M. C. Yee, J. Chem. Phys. **77**, 3578 (1982); J. M. Ugalde, R. J. Boyd, and J. S. Perkyns, *ibid.* **87**, 1216 (1987); E. M. Piexoto, C. R. Bunge, and R. A. Bonham, Phys. Rev. **181**, 322 (1969); R. Benesch and V. H. Smith, Jr., J. Chem. Phys. **55**, 482 (1971).

[11]R. J. Boyd and C. A. Coulson, J. Phys. B **7**, 1805 (1974); G. Sperber, Int. J. Quantum Chem. **5**, 177 (1971), **5**, 189 (1971); see also, V. Maslen, Proc. Phys. Soc. London, Sect. A **69**, 734 (1956); J. Lennard-Jones and J. A. Pople, Philos. Mag. **93**, 581 (1952); R. McWeeny and Y. Mizuno, Proc. R. Soc. London, Ser. A **259**, 554 (1961).

[12]S. R. Gadre and S. J. Chakravorty, J. Chem. Phys. **86**, 2224 (1987); Proc. Indian Acad. Sci. **96**, 241 (1986).

[13]S. R. Gadre, T. Koga, and S. J. Chakravorty, Phys. Rev. A **36**, 4155 (1987).

[14]W. Weyrich, Acta Crystallogr. Sect. A **43**, C320 (1987); W. Weyrich, paper presented at the SAGAMORE workshop on Density Matrices, Coimbra, Portugal, 1988 (unpublished).

[15]E. Clememti and C. Roetti, At. Data Nucl. Data Tables **14**, 177 (1974).

[16]J. A. Alonso and N. H. March, J. Chem. Phys. **78**, 1382 (1983).

[17]Note that only the hydrogenic 1*s* orbitals are rigorously nodeless. In a basis set this is not guaranteed. In fact, the basis set of Ref. 15 for the Be 1*s* HF orbital does exhibit a node around $r=4.5a_0$ (where the value of the function is $\sim 10^{-6}$ a.u.). Whenever the orbital is seen to be significantly deviating from zero after a given node, such a node is termed "prominent."

[18]L. C. Balbás (private communication).

[19]C. A. Coulson and A. H. Neilson, Proc. Phys. Soc. London **78**,

831 (1961).
[20]W. Kutzelnigg, G. Del Re, and G. Berthier, Phys. Rev. **172**, 49 (1968).
[21]R. Ahlberg and P. Linder, J. Phys. B **9**, 2963 (1976); R. J. Mobbs and K. E. Banyard, J. Chem. Phys. **78**, 6106 (1983); G. Doggett, Mol. Phys. **38**, 853 (1979).
[22]D. W. Smith, E. G. Larson, and R. Morrison, Int. J. Quantum Chem. Symp. **3**, 689 (1970); R. Resta, Int. J. Quantum Chem. **14**, 171 (1978); K E. Banyard and R. J. Mobbs, J. Chem. Phys. **75**, 3933 (1981); N. Moiseyev and P. R. Certain, Chem. Phys. Lett. **55**, 451 (1978); A. J. Thakkar and V. H. Smith, Jr., Phys. Rev. A **23**, 473 (1981); A. J. Thakkar, *ibid.* **25**, 1820 (1982); R. K. Pathak, *ibid.* **31**, 2806 (1985).
[23]C. A. Coulson, Proc. Cambridge Philos. Soc. **37**, 55 (1941).